Electrochemical and peroxidase catalysed oxidation of 9-β-D-ribofuranosyluric acid 5′-monophosphate

Rajendra N. Goyal and Arshi Rastogi

Department of Chemistry, University of Roorkee, Roorkee-247 667, India

The electrochemical oxidation of 9-β-D-ribofuranosyluric acid 5′-monophosphate (UA-9R-5′-P) in aqueous solution has been studied in the pH range 2.10–10.0. The evidence strongly indicates that UA-9R-5′-P is oxidized in a $2e^-$, $2H^+$ reaction to give an unstable diimine which subsequently decomposes. A UV absorbing intermediate is observed during electrooxidation which decays in a pseudo first-order reaction to give alloxan, urea and ribosyl phosphate at pH 3.0. Controlled potential electrolysis results in the transfer of 2.0 ± 0.2 electrons per molecule and three major products are obtained at pH 7.0; allantoin, 5-hydroxyhydantoin-5-carboxamide and D-ribose. Tentative reaction schemes are proposed to explain the formation of these products.

Oxidation of UA-9R-5′-P in the presence of peroxidase and H_2O_2 also generates an intermediate which has spectral and kinetic properties identical to those of the intermediate generated electrochemically. Thus, it is believed that electrochemical and enzymic oxidation of UA-9R-5′-P proceed by identical reaction mechanisms.

Introduction

The involvement of purine nucleotides in nucleic acid synthesis and other essential metabolic reactions was realised long ago.[1,2] Purine nucleotides are allosteric effectors of a number of enzymes and thus participate in the intricate processes of metabolic regulation. The presence of the ribosophosphate moiety not only influences conformation involving association but affects electron density at electroactive sites. The electrochemical oxidation of purines, particularly uric acid, in aqueous solutions has been extensively studied by various workers[3–5] and a well-defined oxidation peak was noticed in cyclic voltammetry. However, investigations of purine nucleotides revealed that these compounds do not give a wave in polarography. Palecek[6,7] has reported the anodic indentation for such compounds in oscillographic polarography. The applications of electrochemical techniques in nucleic acid research have also been compiled by Palecek and co-workers.[8] In our continued study into the electrochemical and enzymic oxidation of purines,[9,10] the effect of the ribosophosphate substituent on the redox properties of purines is reported in this paper. As the mechanism of electrochemical and peroxidase catalysed oxidation of uric acid is probably best understood,[11] it was considered interesting to elucidate the effect of the ribosophosphate moiety on uric acid.

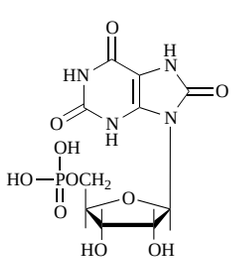

1

9-β-D-Ribofuranosyluric acid 5′-monophosphate (UA-9R-5′-P) does not occur naturally in man. However, it may be isolated from bovine blood and liver.[12] The biosynthesis of 9-β-D-ribofuranosyluric acid 5′-monophosphate (**1**) has been reported[13] in an extract of *Lactobacillus plantarum.* A detailed redox mechanism for the oxidation of UA-9R-5′-P is suggested on the basis of linear and cyclic sweep voltammetry, coulometry, spectral studies and product analysis.

Experimental

9-β-D-Ribofuranosyluric acid 5′-monophosphate was synthesised in the laboratory by the method of Ikehava and Murao.[14] The purity of the synthesised material was established by repeated crystallization and analysis of C, H and N.

Type VIII peroxidase isolated from Horseradish peroxidase (R_z ~ 3.4) was obtained from Sigma Chemical Co., USA and catalase was a product of the CSIR Centre for Biochemicals, New Delhi.

The equipment used for electrochemical studies and spectral studies was essentially the same as that described earlier.[15] The pyrolytic graphite electrode (PGE), glassy carbon electrode (GCE) and platinum electrodes used for the electrochemical studies were fabricated in the laboratory by the method reported earlier[16] and had a surface area of ~9, 12 and 3 mm^2, respectively. The renewal of the platinum and PGE surface after each voltammogram was carried out by polishing on a 600 grit metallographic polishing disc, whereas that of GCE was carried out by the method suggested by Chan and Fogg.[17] All studies were carried out in the phosphate buffers[18] of ionic strength 0.5 M at 22 ± 1 °C. All potentials were measured using the saturated calomel electrode as reference. The value of n, the number of electrons involved in oxidation, was determined by controlled potential electrolysis (CPE) by electrolysing about 30 ml of the solution of compound **1** in a conventional H-cell. The dimensions of the working electrodes were 6 × 1 cm^2, 2 × 2 cm^2 and 6 cm length × 0.25 cm radius for the pyrolytic graphite, platinum and glassy carbon, respectively. The solution was stirred using a magnetic stirrer and nitrogen was continuously bubbled through the solution during CPE. The spectral changes during oxidation and the kinetics of decomposition of the UV absorbing intermediate were monitored in a 1.0 cm quartz cell. IR spectra of the products were recorded as KBr pellets using a Beckmann IR-20 spectrophotometer. TLC was carried out using silica gel-G as adsorbent and acetonitrile–methanol (9:1) as eluent. High performance liquid chromatography was used to separate the products of oxidation at pH 3.0 using LC-10 AD Shimadzu liquid chromatograph equipped with a C_{18} reversed phase column. Methanol was used as the mobile phase and the absorbance of the eluent was monitored at 215 nm. Mass spectra of the products were recorded using a JEOL JMS D300 mass spectrometer.

Procedure

The stock solution (1 mM) of 9-β-D-ribofuranosyluric acid 5′-monophosphate was prepared in double distilled water. The solutions for recording linear and cyclic voltammograms were prepared by mixing 2.0 ml of the stock solution with 2.0 ml of buffer of appropriate pH so that the overall ionic strength of the solution became 0.5 M. Nitrogen gas was bubbled in the solutions for 8–10 min before recording the voltammograms. Although the electrode surface was cleaned after each run, the peak current values showed a variation of ±10%. Hence, for determining the peak current values, an average of at least three runs was taken. The products of electro-oxidation of UA-9R-5′-P were separated at pH 3.0 by using HPLC. For this purpose, the exhaustively electrolysed solution of UA-9R-5′-P was lyophilized. The freeze dried material was dissolved in HPLC grade methanol and filtered to remove the buffer constituents. Methanol was also used as a mobile phase in HPLC. 10 μl of the solution was injected into the HPLC C_{18} column and the flow rate of the mobile phase solvent was fixed at 0.5 ml min^{-1}. The absorbance of the eluent was monitored at 215 nm.

The enzymic oxidation of UA-9R-5′-P was carried out in a 1 cm quartz cell. All the solutions used in enzymic oxidation were prepared in phosphate buffer of desired pH. 2.0 ml UA-9R-5′-P (0.2 mM) was mixed with 0.25 ml horseradish peroxidase (0.002 mM; approx. $M_w \sim 20\,000$). The enzymic reaction was initiated by adding 0.5 ml of H_2O_2 (6 mM) and the spectral changes were recorded. For monitoring the decay of the UV absorbing intermediate generated during enymic oxidation, UA-9R-5′-P was oxidised for 8–10 min. The oxidation was terminated by addition of 0.1 ml catalase (1 mg ml^{-1}). The change in absorbance at selected wavelengths was then monitored. Cyclic voltammograms during enzymic oxidation were also recorded at different times after initiating oxidation by adding hydrogen peroxide.

Silylation of the products was carried out in 3.0 ml vial (Pierce Chemical Co., USA) by heating about 40 μg of the material with 0.1 ml bistrimethylsilyl acetamide (BSA) and 0.1 ml silylation grade pyridine. The vial was tightly closed and heated for 15 min at 110 °C. It was then allowed to cool and then 5 μl were injected into the GC–MS.

Results and discussion

Linear and cyclic sweep voltammetry

Linear sweep voltammetry of 0.1 mM solution of 9-β-D-ribofuranosyluric acid 5′-monophosphate at a sweep rate of 10 mV s^{-1} exhibited one well-defined oxidation peak (Ia). The shape of the peak indicated adsorption complications. In the pH range 2.1–10.0 at PGE and GCE the peak obtained was sharp and spiky in nature whereas at the platinum electrode a broader peak was observed only in the pH range 5.0–8.0. The peak potential (E_p) of the oxidation peak Ia was dependent on pH and shifted to a less positive potential with increasing pH at all the three electrodes used. In the entire pH range, the peak potential at GCE was 40–50 mV more positive than was observed at PGE. The E_p *versus* pH plots at both the electrodes exhibited a break at around pH 6.0 which corresponds to the pK_a of UA-9R-5′-P. The dependence of E_p on pH can be represented by the expressions (1)–(4).

$$E_p\ (\text{pH } 2.1\text{–}6.0) = (0.780 - 0.075\ \text{pH})\ \text{V at PGE} \quad (1)$$

$$E_p\ (\text{pH } 6.0\text{–}10.0) = (0.480 - 0.025\ \text{pH})\ \text{V} \quad (2)$$

$$E_p\ (\text{pH } 2.1\text{–}6.0) = (0.840 - 0.0812\ \text{pH})\ \text{V at GCE} \quad (3)$$

$$E_p\ (\text{pH } 6.0\text{–}10.0) = (0.520 - 0.025\ \text{pH})\ \text{V} \quad (4)$$

The pK_a 6.0 corresponds to proton dissociation from the phosphoric acid group and was similar to the structurally similar adenosine-5′-phosphoric acid where proton dissociation from the phosphoric acid group is well documented.[19,20] Thus, the species that exists in the solution above pH 6.0 is the monoanion. The E_p of the monoanion is also dependent on pH as protons are involved in oxidation.

Table 1 Peak currents observed and peak potentials separation for peaks Ia and Ic for 0.1 mM UA-9R-5′-P at different pH

pH	i_p/μA			
	Ia	Ic	Ia/Ic[a]	$\Delta(Ep^a - Ep^c)$/mV
2.0	10	—	—	—
3.0	10	1.0	10.0	50.0
4.0	11	1.5	7.3	70.0
5.0	12	2	6.5	62.0
6.0	10	2	5	50.0
7.0	12	2.5	4.8	75.0
8.7	8	—	—	—
9.0	6	—	—	—
10.0	8	—	—	—

[a] Average of at least three replicate determinations.

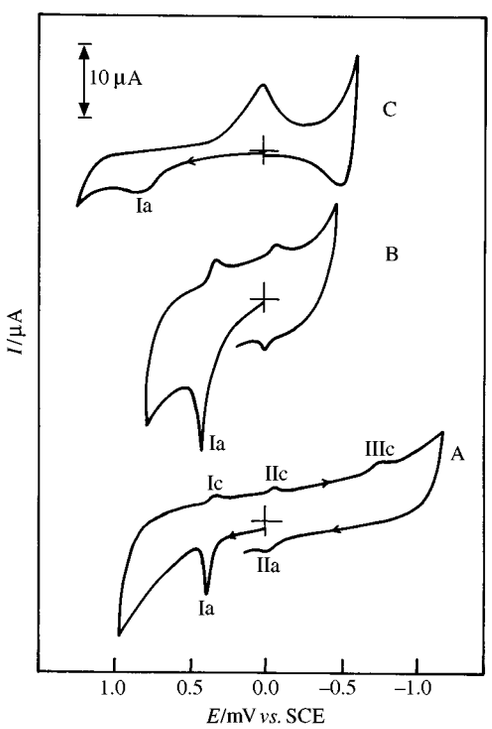

Fig. 1 Typical cyclic voltammogram of 0.1 mM UA-9R-5′-P at pH 5.0 at different solid electrodes. Sweep rate = 100 mV s^{-1}, (*a*) PGE, (*b*) GCE and (*c*) Pt.

Cyclic sweep voltammetry of 9-β-D-ribofuranosyluric acid 5′-monophosphate also exhibited a well-defined oxidation peak (Ia) at a sweep rate of 100 mV s^{-1}, when the sweep was initiated in the positive direction. In the reverse sweep, a well-defined reduction peak (Ic) was noticed in the pH range 3.0–8.0 which formed a quasi-reversible couple with peak Ia, as established by the peak potential separation of the anodic and cathodic peaks. The values of $\Delta(E_p^a - E_p^c)$ were in the range 50–75 mV and are summarised in Table 1. In the pH range 5.0–8.0, two additional reduction peaks (IIc and IIIc) were observed. Peak IIc formed a quasi-reversible couple with peak IIa observed in the subsequent sweep towards positive potentials. Only one reduction peak was noticed at the platinum electrode. A comparison of cyclic voltammograms of 9-β-D-ribofuranosyluric acid 5′-monophosphate at all the three electrodes is presented in Fig. 1.

The peak current of peak Ia was practically independent of pH in the pH range 2.0–8.0 and at pH > 8.0 the peak current slightly decreased. The decrease in peak current at higher pH for peak Ia and its shape suggests the possibility of a lesser

Table 2 Peak currents observed at different sweep rates for the redox couple Ic/Ia of 0.1 mM UA-9R-5′-P at pH 7.0

Sweep rate/mV s^{-1}	i_p/μA		
	Ia	Ic	Ic/Ia[a]
10	2.5	—	—
20	6.0	—	—
50	10.0	1.0	0.10
100	12.0	2.0	0.16
200	25.0	5.0	0.20
300	40.0	7.5	0.18
400	50.0	10.0	0.20
500	55.0	12.5	0.23
600	60.0	15.0	0.25
700	65.0	20.0	0.31

[a] Average of at least three replicate determinations.

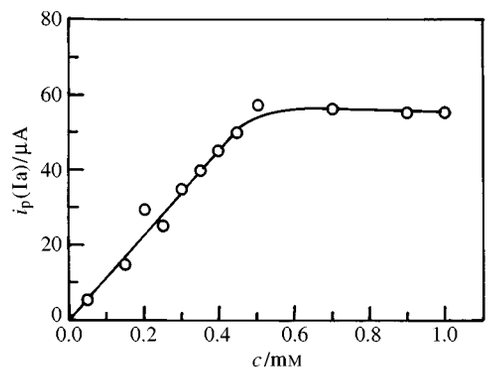

Fig. 2 Dependence of peak current (i_p) on concentration for the oxidation peak Ia at pH 7.0

adsorption at a higher pH. Peak Ic, however, was found to increase with increase in pH and became almost 2.5 times greater at pH 7.0 than the peak current observed at pH 3.0 (Table 1). One of the reasons for such an increase is that the conjugate acid is more easily reduced. Table 1 presents the ratio of peaks Ia/Ic which indicates that the ratio decreased with increase in pH and became constant at pH > 6.0. Peak Ic did not appear at pH > 8.0. This behaviour clearly indicated that the reaction of the species involved in peak Ic is acid–base catalysed. Identical behaviour was noticed at the glassy carbon electrode, whereas peak Ic was never observed at the platinum electrode. The E_p of peaks Ic and IIc shifted to a more negative potential with an increase in pH ($dE_p/dpH \sim 55$ and 50 mV per pH unit, respectively). The peak current for peaks IIa and IIc were more or less constant in the pH range 5.0–8.0 with a ratio IIc/IIa ~ 1.0. The ΔE_p for the redox couple IIc/IIa in the entire pH range was ~50 mV.

The peak current of peak Ia increased with an increase in concentration of UA-9R-5′-P in the concentration range 0.05–1.0 mM at all the three electrodes. The plot of i_p *versus* concentration can be approximated to a straight line in the range 0.05–0.5 mM at the PGE and GCE and then attains a more or less constant value (Fig. 2). At the platinum electrode, the i_p value increased linearly in the entire concentration range used. This behaviour indicated the involvement of adsorption complications[21] in the electrode reaction at the PGE and GCE. The adsorption complications[22] at the PGE and GCE were further confirmed by the increase in peak current function ($i_p/\sqrt{v}$) with increasing sweep rate as shown in Fig. 3.

It was interesting to observe that the peak current of peak Ic increased with an increase in sweep rate in the range 10–700 mV s^{-1} at PGE and GCE. The ratio of peaks Ic/Ia increased with increasing sweep rate and reached to 0.31 at 700 mV s^{-1}. This behaviour indicated that the species involved in the reduction of peak Ic is unstable and hence is more available at higher sweep rates (Table 2), which is most probably due to competitive chemical reactions.[23,24] The potential of peak Ia was also found

Table 3 Experimental *n* values observed for 0.1 mM UA-9R-5′-P at different solid electrodes

pH	Electrode	*E*/V *vs.* SCE	*n*[a]
2.0	PGE	0.75	1.82
	GCE	0.75	1.86
4.0	PGE	0.60	1.94
	GCE	0.60	2.02
6.0	PGE	0.50	1.96
7.0	PGE	0.50	2.02
	GCE	0.50	2.08
8.7	PGE	0.40	2.02
	GCE	0.40	1.92
10.0	PGE	0.40	2.10
	GCE	0.40	1.90

[a] Average of at least three replicate determinations.

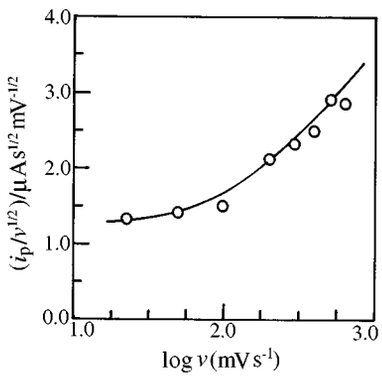

Fig. 3 Dependence of $i_p/\sqrt{v}$ *versus* log *v* observed for peak Ia of 0.1 mM UA-9R-5′-P at pH 7.0

to shift to a more positive potential with an increase in sweep rate in the range 10–700 mV s^{-1} at the PGE and GCE. For systems complicated by adsorption, dependence of E_p on *v* has no simple meaning. However, in the sweep range 10–200 mV s^{-1}, the values of E_p shifted by 15–20 mV per ten-fold increase in the sweep rate, whereas at a higher sweep rate, the value decreased to 8–10 mV. The plots of $(\Delta E_p/2)/\Delta\log V$ *versus* log *v* were S-shaped at both the electrodes.

The value of *n*, the number of electrons involved in oxidation of 9-β-D-ribofuranosyluric acid 5′-monophosphate in the concentration range 0.1–0.5 mM was determined at different electrodes by controlled potential electrolysis. The peak current for peak Ia decreased exponentially with time. However, the log i_p *versus* time plots were linear only for the first 10–15 min of oxidation, and thereafter a large deviation from the straight line was observed. During the first 10–15 min about 18–20% conversion of compound **1** was achieved. This behaviour suggested that the electrode reaction followed a simple path only for the first 10–15 min of oxidation and after that the competitive follow-up chemical reactions play a significant role as suggested by Cauquis and Parker[25] and Meites.[26] The *n* values determined at different pH at the PGE and GCE were found to be 2.0 ± 0.2 and are summarized in Table 3.

Spectral studies

The spectral changes during electrooxidation of 9-β-D-ribofuranosyluric acid 5′-monophosphate were monitored at pH 3.0, 5.0 and 7.0. A UV spectrum of 0.1 mM UA-9R-5′-P at pH 3.0 is presented just before electrolysis by curve 1 in Fig. 4(A) and exhibits three well-defined maxima at 288, 234 and 201 nm. Upon application of a potential 100 mV more positive to peak Ia at GCE, the absorbance at λ_{max} systematically decreased, whereas the absorbance in the region 200–225 nm increased systematically (curves 1–6). If the potential is turned off at any stage of oxidation, a systematic decrease in absorbance in the region 215–290 nm is observed. Fig. 4(B) presents changes observed after turning off the potential after recording

Table 4 Observed rate constants for the decomposition of the UV absorbing intermediate generated during electrooxidation of 0.1 mM UA-9R-5′-P

		$k/10^{-3}$ s^{-1}	
pH	λ/nm	Electrochemical	Enzymatic
3.0	287	2.540	—
	258	2.280	—
	233	1.160	—
5.0	294	1.440	1.859
	240	1.310	1.893
	222	1.360	1.443
7.0	294	1.064	—
	240	1.087	1.131
	222	1.188	1.568

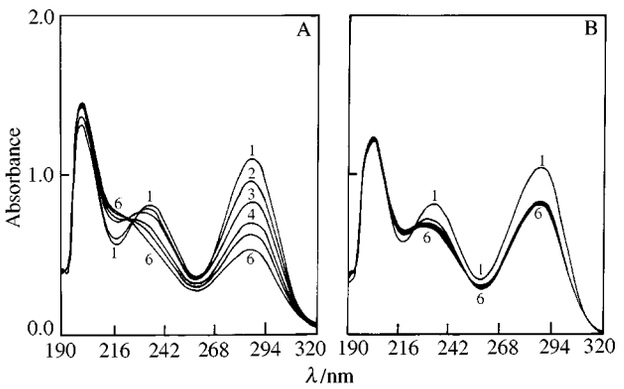

Fig. 4 (A) Spectral changes observed during electrooxidation of 0.1 mM UA-9R-5′-P at pH 3.0; $E = 1.2$ V *vs.* SCE. Curves were recorded at an interval of 10 min (1–6). (B) Spectral changes observed after turning off the potential corresponding to curve 3 in Fig. 4(A). Curves were recorded at an interval of 10 min.

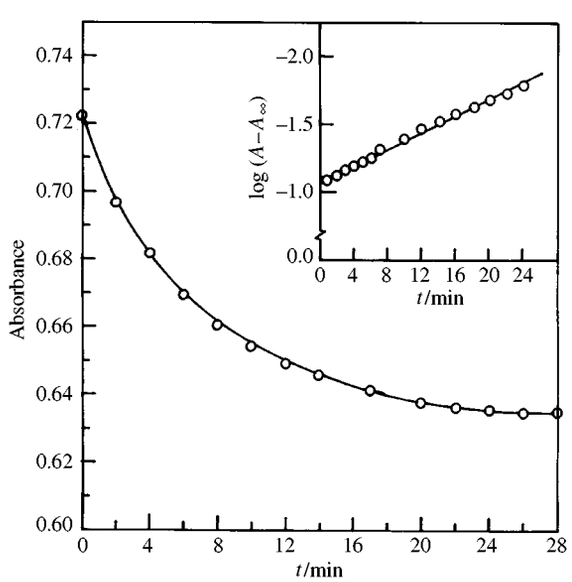

Fig. 5 *A vs. t* and log $(A - A_\infty)$ *vs. t* plots observed at 233 nm at pH 3.0 for the decay of the UV absorbing intermediate generated during electrooxidation of I

curve 3 in Fig. 4(A). The decrease in absorbance in the region 215–250 nm was larger in comparison to the region 250–290 nm. The apparent maximum at 201 nm is caused by an increase in absorbance (A) with decreasing λ and by the decrease in the signal due to instrumental features and has probably no physical meaning. The true λ_{max} for the process at $\lambda < 210$ nm is probably smaller than 190 nm. This is supported by Fig. 4(B) which shows that no change in A_{200} occurs when both A_{240} and A_{290} decrease. The stirring was completely stopped before

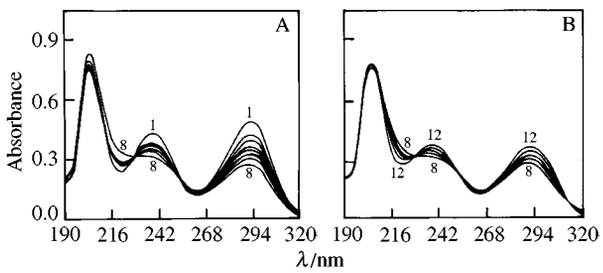

Fig. 6 (A) Observed spectral changes during electrooxidation of 0.1 mM UA-9R-5′-P at pH 5.0, $E = +1.0$ V *vs.* SCE. (B) Observed spectral changes after turning the potential to -1.0 V *vs.* SCE after recording curve 8 in Fig. 6A. Curves were recorded at an interval of 5 min.

recording curve I in Fig. 4(B). The decay in absorbances at selected wavelengths were monitored with time and the resulting curves were exponential in nature (Fig. 5). The value of the pseudo first-order rate constants (k) have been calculated from the linear plots of log $(A - A_\infty)$ *vs.* time plots and are presented in Table 4. It was interesting to observe that the value of k at pH 3.0 was almost twice than observed at pH 5.0 and 7.0. Thus, it seems reasonable to conclude that the rate of follow-up chemical reactions at pH 3.0 is faster in comparison to pH 5.0 and 7.0.

Spectral changes in the pH range 5.0–8.0 (where peak IIIc was clearly observed) were also monitored when oxidation at peak Ia was followed by reduction at peak IIIc potentials. Fig. 6(A) presents the spectral changes which occur upon electrooxidation of 9-β-D-ribofuranosyluric acid 5′-monophosphate at pH 5.0. Thus, the absorbance systematically decreases at both the λ_{max} and an increase is observed in the range 205–230 nm. If the potential is shifted to -0.8 V after recording curve 8 in Fig. 6(A), spectral changes shown in Fig. 6(B) are observed. The absorbance at both the λ_{max} started increasing and the absorbance in the region 205–230 nm systematically decreased. No definite pattern of increase or decrease was observed at 204 nm. However, it was interesting to observe that curve 12 was basically similar to the UV spectrum of the starting material. Thus, reduction at peak IIIc potentials causes regeneration of the starting material.

Product analysis

The products of electrooxidation of 9-β-D-ribofuranosyluric acid 5′-monophosphate formed in CPE were characterised at pH 3.0 and 7.0 at pyrolytic graphite and glassy carbon electrodes. The products formed during the CV on a microelectrode can always differ from the product formed by CPE at a large surface electrode. At pH 3.0, the exhaustively electrolysed solution of UA-9R-5′-P was lyophilised and the colourless freeze-dried material was treated with methanol. The filtered methanolic solution of the products was analysed by HPLC. Fig. 7 presents the HPLC chromatogram observed and shows three major peaks at retention times (R_t) 4.4, 5.9 and 6.5 min, respectively. The small peak at $R_t \sim 7.9$ min was found to be due to the starting material by comparison of the R_t with that of the authentic sample. To collect the material under HPLC peaks 1, 2 and 3, several injections were made and the volume was collected. The colourless, dried material obtained under each peak was characterised by mp, IR, ^{1}H NMR and mass spectra.

HPLC Peak 1. The white material obtained under this peak showed a single spot in TLC ($R_f \sim 0.36$) and had a mp 238 °C. The IR spectrum of the material gave strong bands at 1720, 1635, 1400, 1250, 1170, 1020, 800 and 775 cm^{-1}. The ^{1}H NMR spectrum of the material exhibited two signals at $\delta = 11.2$ (s, NH) and 11.6 (s, NH) and hence the material was characterised as alloxan. Further confirmation of alloxan was also made by recording the IR spectrum of authentic alloxan.

HPLC Peak 2. The white material obtained exhibited only a single spot in TLC ($R_f \sim 0.70$) and had a mp 134 °C. The FTIR

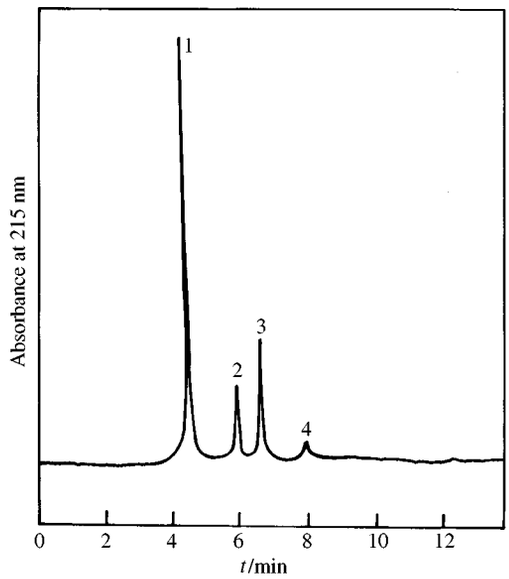

Fig. 7 HPLC chromatogram observed for the electrooxidation products of 9-β-D-ribofuranosyluric acid 5′-monophosphate at pH 3.0

spectrum of the material gave sharp bands at 3385, 3490 and 1675 cm^{-1} and this spectrum was practically superimposable on that of an authentic urea sample. Hence, it was concluded that the material obtained under this peak is urea. The formation of urea was further confirmed by recording the mass spectrum of the material and a clear molecular ion peak at $m/z = 60$ (100%) was observed.

HPLC Peak 3. The small amount of material obtained under this peak did not permit its complete characterization. It had a mp > 250 °C and exhibited a single spot in TLC ($R_f \sim 0.36$). The mass spectrum of the material exhibited a clear molecular ion peak at m/z 230 (11.6%) and hence it was concluded that the material is ribosyl phosphate. Thus, the major products of oxidation of 9-β-D-ribofuranosyluric acid 5′-monophosphate at pH 3.0 are alloxan, urea and ribosyl phosphate.

The products of electrooxidation of 9-β-D-ribofuranosyluric acid 5′-monophosphate at pH 7.0 were separated by gel permeation chromatography (see Experimental). The first peak between volume 140–180 ml was found to contain phosphate and hence was discarded. Four other peaks P_2 (200–220 ml), P_3 (240–260 ml), P_4 (260–290 ml) and P_5 (330–340 ml) were separately collected and lyophilised. Peak P_4 was slightly overlapping with peak P_3 and hence the volume overlapped was collected with peak P_4. The colourless material obtained under peak P_2 had a mp 89 °C. It exhibited prominent bands in the IR spectrum at 3910, 3774, 3666, 3470, 3304, 3093, 3047, 2843, 2603, 2480, 2405, 2332, 2177 and 1636 cm^{-1}. The molar mass of the material was 150 (82.6%) and hence this product was characterised as ribose. A further confirmation of the formation of ribose was also made by recording the IR spectrum of the authentic ribose. The IR spectrum of the authentic D-ribose was practically superimposable on the IR spectrum obtained for the material.

The fluffy white material obtained under chromatographic peak P_3 had a mp 230 °C and exhibited only a single spot in TLC ($R_f \sim 0.34$). The ^1H NMR spectrum of the material exhibited signals at δ 5.26 (d, 1H), 5.80 (s, 3H), 8.00 (s, 1H) and 10.48 (s, 1H) and hence suggested the material to be allantoin. The mass spectrum of the material exhibited a clear molecular ion peak at m/z 158 (62.1%) which further confirmed the material as allantoin. Some other high mass peaks observed in the fragmentations pattern were at 141 (8.0%), 140 (5.2%), 130 (28.2%), 129 (4.1%), 116 (2.8%) and 115 (15.8%).

The colourless material obtained under chromatographic peak P_4 always showed two spots in TLC ($R_f \sim 0.34$ and 0.44) due to overlapping of peaks P_3 and P_4. As separation by gel

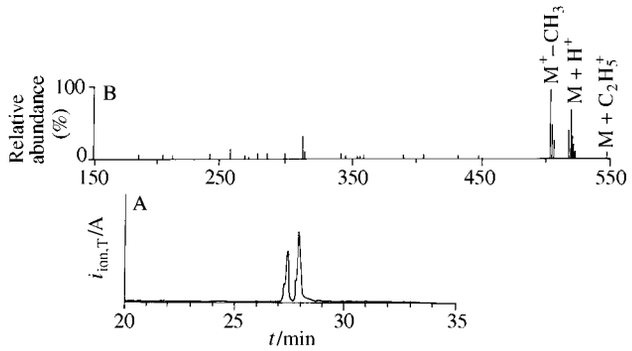

Fig. 8 (A) Total ion current chromatogram observed for the products eluted under peak P_4 in gel permeation chromatography. (B) Chemical ionization mass spectrum observed for the peak at $R_t > 27.2$ min.

permeation chromatography could not be achieved, it was considered desirable to characterize the product responsible for peak P_4 by GC–MS. The silylated sample (see Experimental section) on analysis by GC–MS exhibited two well-defined peaks with $R_t \sim 27.0$ and 30.2 min. The EI mass spectrum of the peak at $R_t \sim 27.0$ min showed a very small ion at $m/z = 518$ (10.4%). The molar mass of the ion as 518, was further confirmed by recording the chemical ionization (CI) mass spectrum of the sample. The CI mass spectrum [Fig. 8(A)] also exhibited two signals at $R_t \sim 27.2$ and 28.1 min. The peak corresponding to $R_t \sim 27.2$ gave a clear signal for $(M + H)^+$ at 519 (70.7%) and $(M - CH_3)^+$ at 503 (100%) and hence confirmed the molar mass of the material as 518. The detailed CI mass spectrum

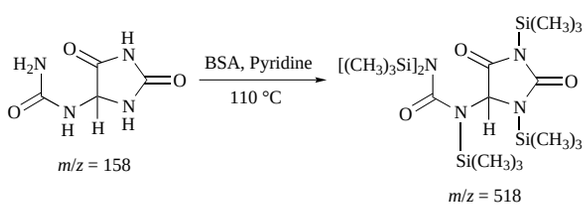

pattern observed is presented in Fig. 8(B) and the molar mass of 518 is assigned to the pentasilylated allantoin.

The peak at $R_t \sim 28.1$ min gave a clear molecular ion peak at $m/z = 447$ (46.8%) which corresponds to tetrasilylated 5-hydroxyhydantoin-5-carboxamide. As 5-hydroxyhydantoin-5-carboxamide has been observed as the product of oxidation of uric acid at pH > 5.0, it appears that the ribosyl phosphate unit is detached during oxidation of 9-β-D-ribofurnosyluric acid 5′-monophosphate. The CI mass spectrum further confirmed the molar mass as being 447 as peaks for $(M + H)^+$ 448 (6.8%),

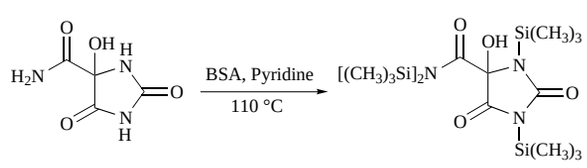

$(M - CH_3)^+$ at 432 (25.4%) and $(M + C_2H_5)^+$ at 476 (11.8%) were observed.

Gel permeation chromatographic peak P_5 was well separated from peak P_4 and hence the material obtained under this peak exhibited only a single spot in TLC ($R_f \sim 0.21$). The material did not melt below 250 °C and exhibited a clear molecular ion peak at m/z 370 (8.6%). The molar mass of 370 corresponded to allantoin attached to the ribosyl phosphate unit. Thus, it is believed that the ribosyl phosphate unit partially hydrolyses to give allantoin, ribose and phosphate at pH 7.0. The other high mass peaks observed in the fragmentation pattern were at m/z

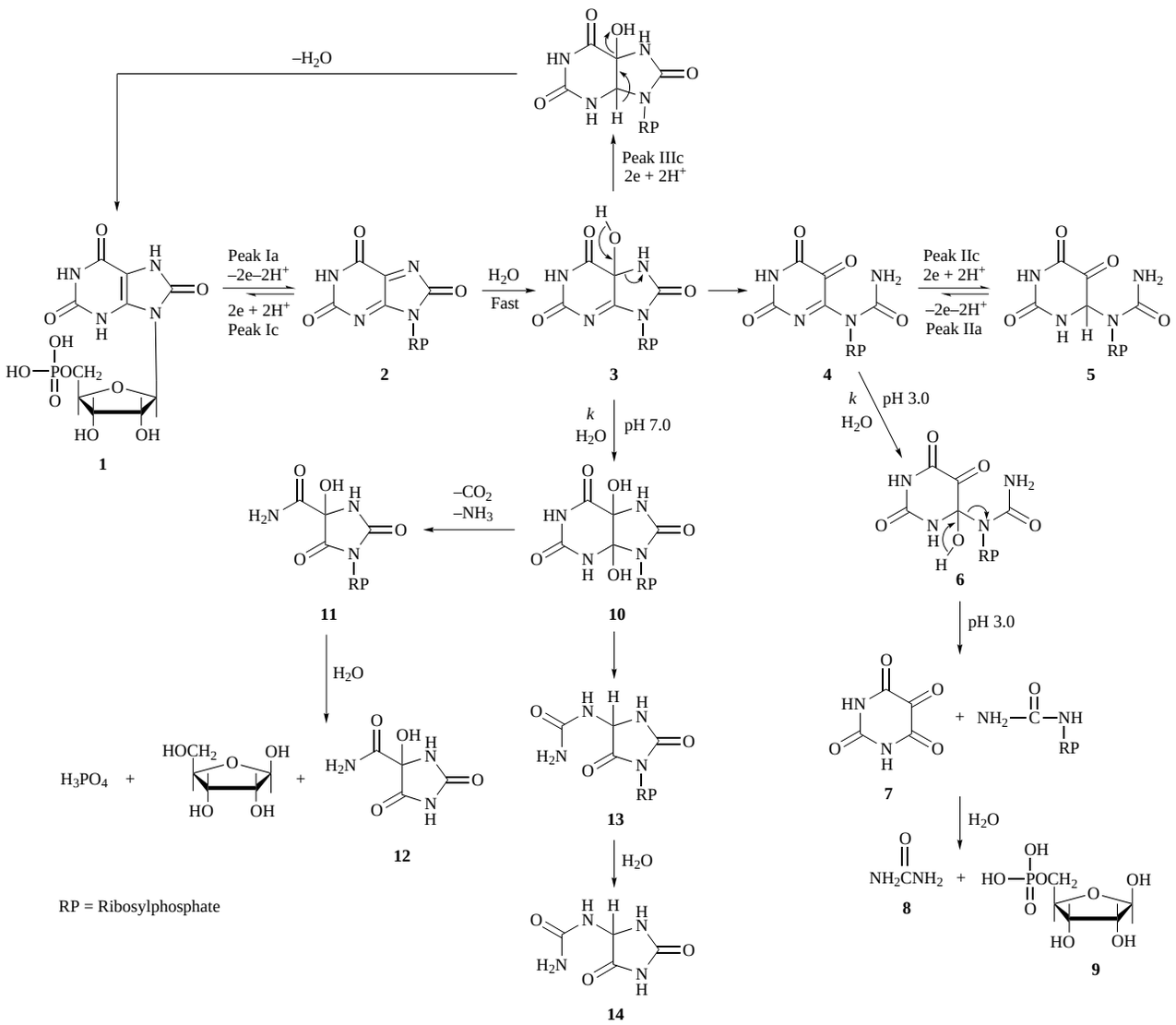

Scheme 1 Tentative mechanism proposed for the oxidation of 9-β-D-ribofuranosyluric acid 5′-monophosphate

352 (4.1%), 312 (4.0%), 282 (1.3%), 277 (1.8%), 254 (2.2%), 166 (16.2%), and 148 (47.7%).

Enzymic oxidation

The peroxidase catalyzed oxidation of 9-β-D-ribofuranosyluric acid 5′-monophosphate was also studied in phosphate buffers of pH 5.0 and 7.0. Spectral changes observed during peroxidase catalyzed oxidation of compound **1** at pH 5.0 are presented in Fig. 9. Curve 1 in Fig. 9 is the UV spectrum of a 0.1 mM aqueous solution of 9-β-D-ribofuranosyl uric acid 5′-monophosphate at pH 5.0 containing horseradish peroxidase and three absorption bands were observed at λ_{max} 290, 238 and 205 nm. When the oxidation was catalyzed by adding hydrogen peroxide, a systematic decrease in absorbance at the λ_{max} was observed (curves 2–14). The absorbance in the region 215–225 nm first increased and then decreased. If enzymic oxidation is terminated by adding catalase, a systematic decrease at 290 and 238 nm was observed. Thus, spectral changes during and after the oxidation were essentially similar to those observed during electrochemical oxidation. To monitor the kinetics of decay of the UV absorbing intermediate generated during enzymic oxidation, 0.5 ml of catalase (1 mg ml^{-1}) was added after recording curve 6 in Fig. 9. This amount of catalase was sufficient to cease the enzymic oxidation and the change in absorbance with time was monitored at a selected wavelength. The absorbance *versus* time plots were exponential in nature and suggested the pseudo first-order nature of the reaction. The values of k were calculated from log $(A - A_\infty)$ *versus* time plots

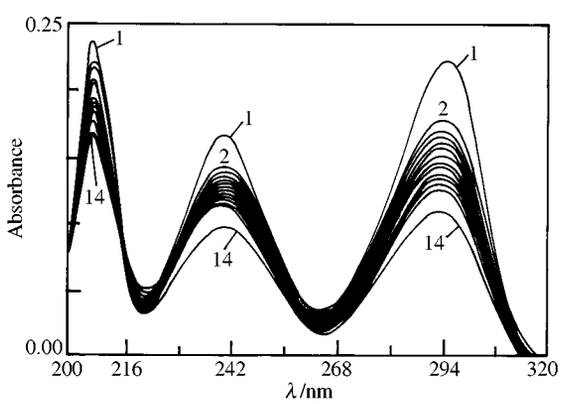

Fig. 9 UV spectral changes observed during enzymic oxidation of 0.1 mM UA-9R-5′-P. Curves were recorded at an interval of 3 min.

and are summarised in Table 4. It is interesting to observe that the values of rate constants observed for electrochemical and enzymic oxidation are practically identical.

Reaction mechanism

On the basis of experimental results presented above, it is possible to suggest a tentative mechanism for the electrochemical and enzymic oxidation of 9-β-D-ribofuranosyluric acid 5′-monophosphate (Scheme 1). The electrochemical oxidation occurred in a single $2e^-$, $2H^+$ reaction. The main argument

favouring a single step oxidation is the value of n. The absence of two separate $1e^-$ peaks is most likely due to deprotonation following the first electron uptake and producing a strongly reducible species is so fast in water that it cannot be out-run in cyclic voltammetry. It is difficult to decide whether enzymic oxidation is a single $2e^-$ step or two $1e^-$ steps. The oxidation of uric acid by peroxidase and uricase in sequential $1e^-$ steps has been reported in the literature.[26–28] The E_p–pH dependence clearly suggests that the electroactive species is a monoanion. The oxidation of **1** in a $2e^-$ step leads to the formation of an unstable diimine species **2**. At PGE and GCE, the reverse peak Ic was observed and the redox couple Ia/Ic was quasi-reversible in nature. The diimine **2** formed is expected to be unstable as has been observed in the case of uric acid[29] and other purines[30,31] and hence would be readily attacked by water in a chemical follow-up step. The attack of $H_2PO_4^-$ on diimine as suggested by Chan and Dryhurst[32] has been ruled out on the basis of recent studies reported in the literature.[33] Thus, the attack of water molecule on **2** gives imine alcohol **3** which seems to be the UV absorbing intermediate of the reaction. Peak IIIc observed in the pH range 5.0–8.0 appears to be due to the reduction on N=C– linkage in imine alcohol **3**. The loss of water from **3** regenerates the starting material **1** as has been confirmed by the oxidation followed by reduction studies. The loss of a proton from the OH group in species **3** causes rupture of the imidazole ring to yield **4**. The attack of one more molecule of water on **3** readily causes saturation of other –N=C– linkage to give **6** which decomposes at pH 3.0 to give alloxan **7**, urea and an ribose phosphate unit. The redox couple IIc/IIa observed in the pH range 5.0–8.0, thus seems to be due to the reduction of –C=N– in species **4** to give dihydro moiety **5**. The imidazole ring opening reactions in purines in acidic medium are not uncommon and have been observed during chemical oxidation by variety of reagents.[34]

At pH 7.0, the attack of a water molecule on imine alcohol **3** readily gives diol **4**. The pyrimidine ring then opens and in a series of steps involving decarboxylation, deamination, the ultimate products obtained are 5-hydroxyhydantion-5-carboxamide **12**, ribose and allantoin **14**. The characterization of allantoin ribosyl-5′-monophosphate **13** by gel permeation chromatography indicated that it hydrolyses to give allantoin **14**. The rupture of the pyrimidine ring of purines in neutral and alkaline medium has also been well-documented in the literature.[35]

The presence of ribosyl phosphate group thus seems to ease the oxidation of uric acid. A comparison of E_p of uric acid and 9-β-D-ribofuranosyluric acid 5′-monophosphate indicated that in the latter the E_p shifts to less positive potential by 50–80 mV in the entire pH range. In the case of uric acid the electroactive species is the monoanion formed by the loss of proton from position 9, whereas in compound **1**, the monoanion is formed from the phosphoric acid group. Redox couple IIc/IIa was never observed in the case of uric acid.

The UV absorbing intermediate was observed in both the compounds at almost the same wavelength region[11] and the values of k were also more or less same. The formation of products in both the cases is in accordance with the properties of purines. It must however, be realized that there is always more than one possible pathway for the formation of observed products. The proposed scheme must be regarded as the most probable pathway and explains all the results obtained. A comparison of electrochemical and enzymic oxidation of 9-β-D-ribofuranosyluric acid 5′-monophosphate clearly indicated that both the oxidation proceeded by the same mechanism.

References

1 F. A. Schultz and I. Taniguchi, *Redox Mechanism and Interfacial Properties of Molecules of Biological Importance*, The Electrochemical Society, Pennington, NJ, 1993, vol. 93.
2 K. J. Volk, R. A. Yost and A. B. Toth, *Anal. Chem.*, 1992, **64**, 21A.
3 G. Dryhurst and P. K. De, *Anal. Chim. Acta*, 1971, **58**, 163.
4 D. L. Smith and P. J. Elving, *Anal. Chim.*, 1962, **34**, 930.
5 G. Dryhurst, *J. Electrochem. Soc.*, 1969, **116**, 1411.
6 E. Palecek, *Nature*, 1960, **188**, 656.
7 E. Palecek, *Prog. Nucleic Acid Res. Mol. Biol.*, 1969, **9**, 31.
8 M. Vorlickova, G. Jezkova, V. Brabec, Z. Pechan and E. Palecek, *Stud. Biophys.*, 1970, **24**, 131.
9 R. N. Goyal, A. K. Jain and N. Jain, *J. Chem. Soc.*, *Perkin Trans. 2*, 1996, 1153.
10 R. N. Goyal, A. Kumar and A. Mittal, *J. Chem. Soc.*, *Perkin Trans. 2*, 1991, 1369.
11 G. Dryhurst, K. M. Kadish, F. Scheller and R. Renneberg, *Biol. Electrochem.*, 1982, **1**, 279.
12 R. Falconer and J. M. Gulland, *J. Chem. Soc.*, 1939, 1369.
13 D. Hatfield, R. A. Greenland, H. L. Stewart and J. B. Wyngaarden, *Biochim. Biophys. Acta*, 91, 160.
14 M. Ikehava and K. Murao, *Chem. Pharm. Bull.*, 1968, **16**, 1330.
15 R. N. Goyal, A. K. Jain and N. Jain, *J. Chem. Soc.*, *Perkin Trans. 2*, 1995, 1061.
16 R. N. Goyal, S. K. Srivastava and R. Agarwal, *Bull. Soc. Chem. Fr.*, 1985, **41**, 281.
17 H. K. Chan and A. G. Fogg, *Anal. Chem. Acta*, 1979, **105**, 423.
18 G. D. Christian and W. C. Purdy, *J. Electroanal. Chem.*, 1962, **3**, 363.
19 E. R. Tucci, Br. E. Doody and N. C. Li, *J. Am. Chem. Soc.*, 1961, **65**, 1571.
20 R. M. Smith and R. A. Alberty, *J. Phys. Chem.*, 1956, **60**, 180.
21 R. S. Nicholson and I. Shain, *Anal. Chem.*, 1964, **36**, 706.
22 R. H. Wopschall and I. Shain, *Anal. Chem.*, 1967, **39**, 1514.
23 P. H. Reiger, *Electrochemistry*, Prentice Hall, NJ, 1987, p. 343.
24 E. C. Brown and R. F. Large, in *Techniques of chemistry*, ed. A. Weissberger and R. W. Rossiter, Wiley, New York, 1974, 423.
25 G. Cauquis and V. D. Parker, *Organic Electrochemistry*, ed. M. M. Baizer, Marcel Dekker, New York, 1973, p. 134.
26 L. Meites, in *Physical methods of chemistry*, ed. A. Weissberger and B. W. Rossiter, Wiley, New York, 1971.
27 R. Bentley and A. Neuberger, *Biochem. J.*, 1952, **52**, 694.
28 K. G. Paul and Y. Avi-Dor, *Acta Chem. Scand.*, 1954, **8**, 637.
29 G. Dryhurst, *J. Electrochem. Soc.*, 1972, **119**, 1559.
30 R. N. Goyal, A. B. Toth and G. Dryhurst, *J. Electroanal. Chem.*, 1982, **131**, 181.
31 A. B. Toth, R. N. Goyal, M. Z. Wrona, T. Lacava, N. T. Nguyen and G. Dryhurst, *Bioelectrochem. and Bienerg.*, 1981, **8**, 413.
32 T. R. Chan and G. Dryhurst, *J. Electroanal. Chem.*, 1984, **177**, 149.
33 R. N. Goyal, A. Mittal and D. Agarwal, *Can. J. Chem.*, 1994, **72**, 1997.
34 E. Shaw, *J. Org. Chem.*, 1962, **27**, 883.
35 V. H. Bredereck, F. Effenberger and G. Rainer, *Ann. N.Y. Acad. Sci.*, 1964, **673**, 82.

Paper 7/01601H
Received 7*th March* 1997
Accepted 25*th June* 1997